

Development of ECE Side Impact MDB Model using Shell Elements

Yoshiki Takahira, Shigeki Kojima
TOYOTA TECHNICAL DEVELOPMENT CORPORATION
1-21, Imae, Hanamoto-cho, Toyota, Aichi, 470-0334, Japan

Tsuyoshi Yasuki, Shinichiro Taki
Toyota Motor Corporation
1, Toyota-cho, Toyota, Aichi, 471-8572, Japan

Summary:

This paper describes the development of a new side impact moving deformable barrier finite element model that uses shell elements for aluminum honeycomb. In a previous study, the new modeling method for aluminum honeycomb was applied to an ODB model and the prediction accuracy of the offset frontal collision analysis was improved. In this study, the new modeling method was applied to the ECE MDB model and a full vehicle crash analysis was performed. The result of a side impact analysis with the new MDB model showed better correlation with test results than with modified material type-126 solid elements.

Keywords:

Automotive Crashworthiness, Side Impact Collision, MDB, Aluminum Honeycomb

1 Introduction

In side impact analyses to predict the vehicle deformation and occupant injury values, it is essential for the moving deformable barrier (MDB) model to replicate the compressive property of aluminum honeycomb. In the past, aluminum honeycomb has been modeled using solid elements, and the prediction accuracy of FEM analysis has been improved by reducing the size of elements and by improving the material model.

This paper describes the development of a new MDB model that uses shell elements for aluminum honeycomb in order to further improve the prediction accuracy of FEM analysis. A honeycomb compressive strength was verified in a barrier impact analysis, and the prediction accuracy of the deformed shape of the vehicle and the MDB was verified in a full vehicle side impact analysis.

2 Technical issue of side impact analyses

2.1 Overview of solid element MDB model

Fig.1 shows an aluminum honeycomb model uses solid elements for ECE R95 progressive MDB model, which has been previously developed. An aluminum honeycomb of the MDB is modeled using 10mm mesh solid elements, with the entire model comprising 440,000 elements. The material model for the aluminum honeycomb is MAT 126 with extended functions that can consider the directional dependency of the compressive strength. (Fig.2)

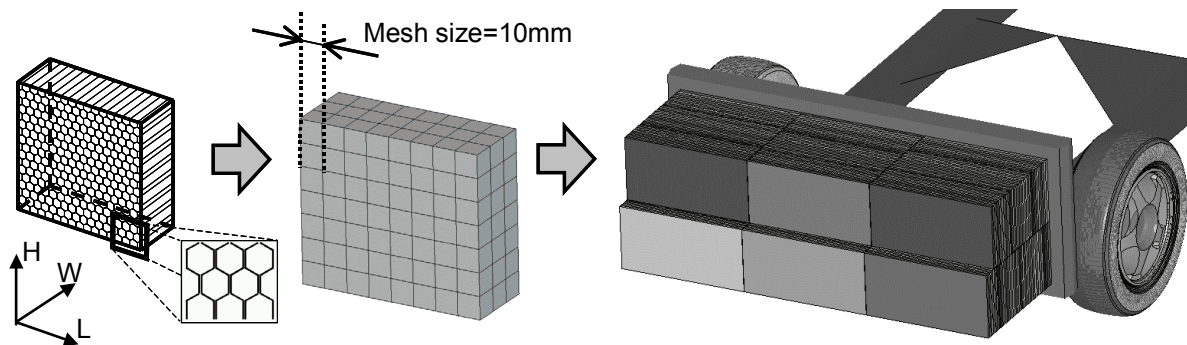


Fig.1 Aluminum honeycomb model using solid elements for ECE R95 MDB model

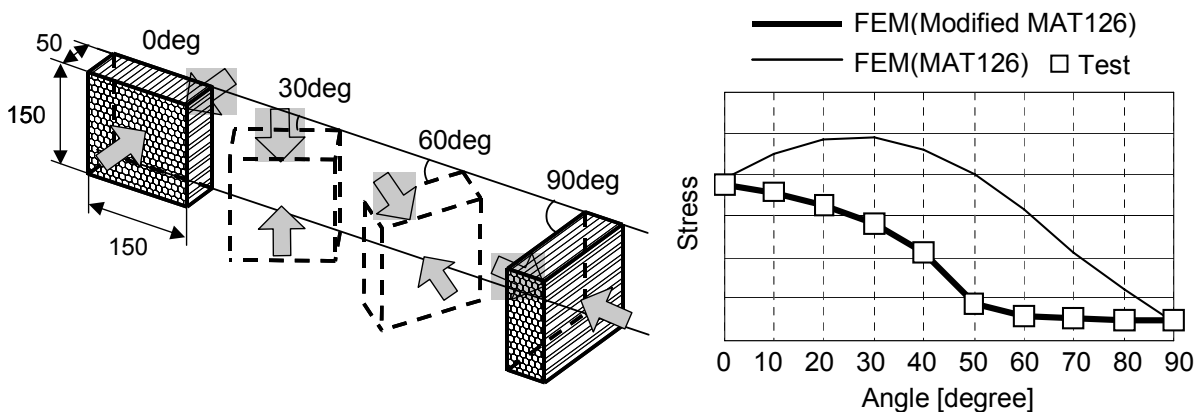


Fig.2 Directional dependency of the aluminum honeycomb compressive strength

2.2 Comparison of test results and FEM analyses for MDB barrier impacts

To verify the compressive strength of the solid element MDB model, FEM analyses were performed on the flat barrier impact and the offset pole impact that had been carried out by EEVC. Fig.3 (a) shows the flat barrier impact model, and (b) shows the relationship between the stroke and the barrier force. Fig.4 (a) shows the offset pole impact analysis model, and (b) shows the relationship between the stroke and the barrier force.

In the flat barrier impact analysis, the relationship between the stroke and the barrier force generally matched the test result. Therefore, it is estimated that the compressive strength of the aluminum honeycomb under axial compression is accurate. On the other hand, the barrier force in the offset pole impact analysis is calculated greater than the test result and the stroke is 32 mm less than the test result.

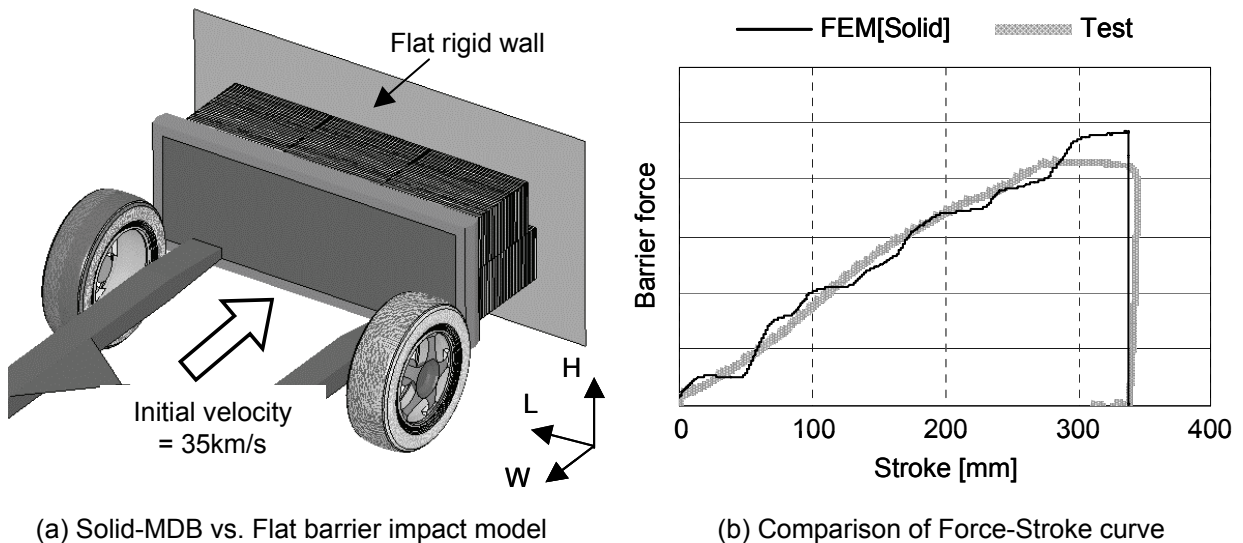


Fig.3 EEVC MDB-flat barrier impact

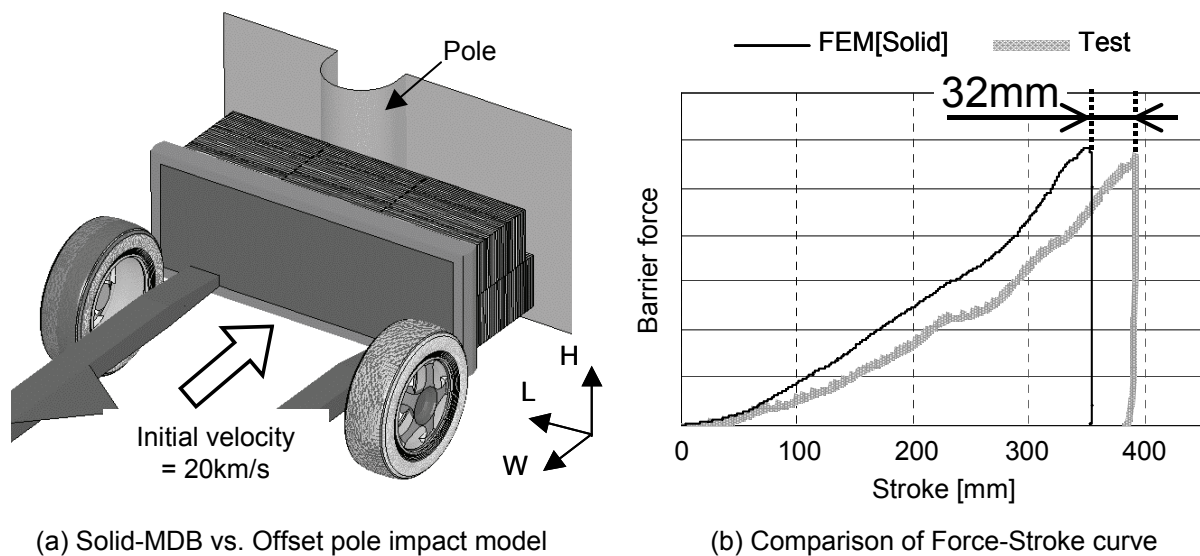


Fig.4 EEVC MDB-offset pole impact

2.3 Difference in the barrier force in the MDB-offset pole impact analysis

This section examines the cause of the difference in the barrier force in the offset pole impact. Fig.5 shows the deformed shape of the aluminum honeycomb near the pole, Fig.6 shows a deformation image of solid elements predicted by the FEM analysis and Fig.7 shows the time history of energy in the region A.

An hourglass energy equivalent to approximately 60% of the total energy is generated in the region A. One of the causes of the difference with the test result is the hourglass control for solid elements. It was therefore concluded that excessive strength that was caused by hourglass control made barrier force high.

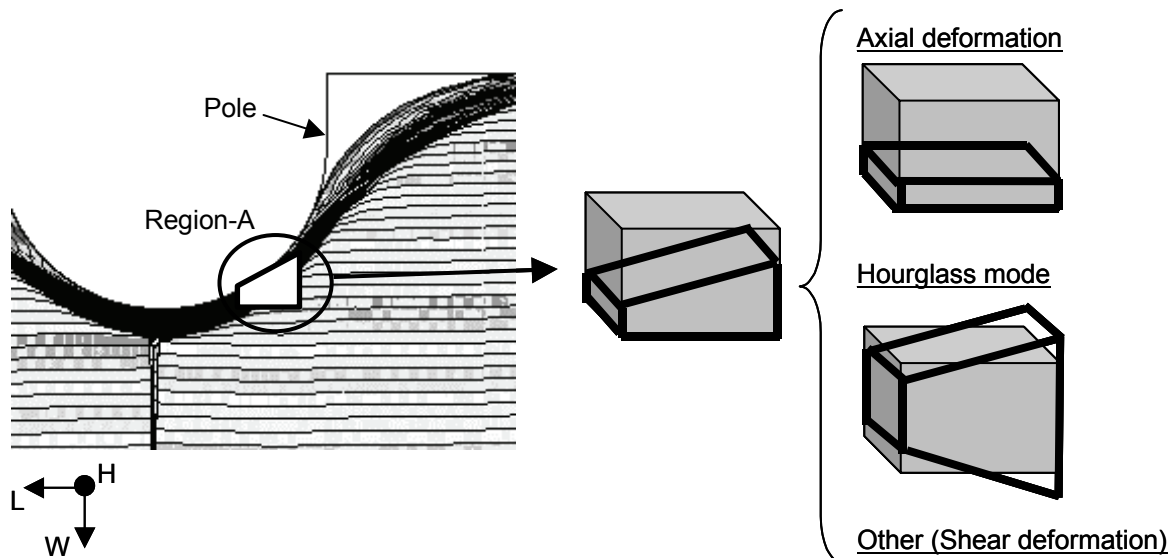


Fig.5 Deformed shape of the honeycomb near the pole Fig.6 Deformation image of the solid element

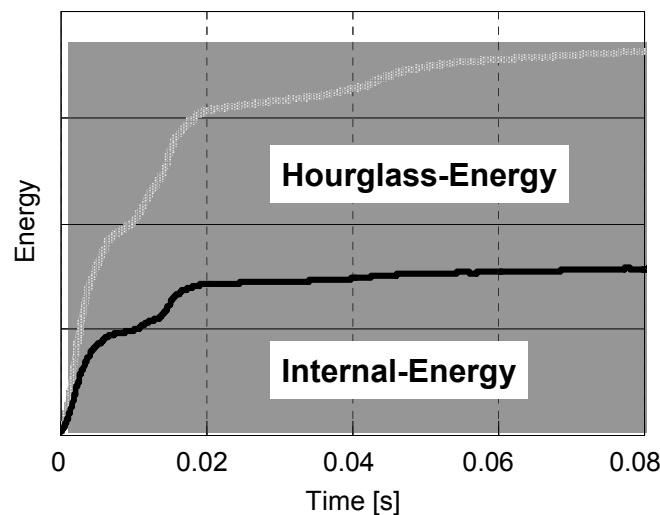


Fig.7 Time history of energy in the region A

3 Modeling of aluminum honeycomb using shell elements

To avoid the hourglass control for solid elements, the modeling of aluminum honeycomb was performed using shell elements. Fig.8 shows the newly developed shell element MDB model. The actual cell size of aluminum honeycomb is 19 mm. In the FEM model, the cell size was increased to 34.6 mm, in order to reduce the number of elements. The minimum length of a shell element was set at 5 mm, in order to enable analyses within a practical CPU time. To approximate the shape of the actual part, pre-crashed areas were applied at the ends of the MDB honeycomb.

Increasing the cell size of the aluminum honeycomb model causes a difference with the actual part in terms of the compressive strength. Therefore, a virtual thickness distribution of the shell elements was defined in order to reproduce the compressive strength of the actual aluminum honeycomb.

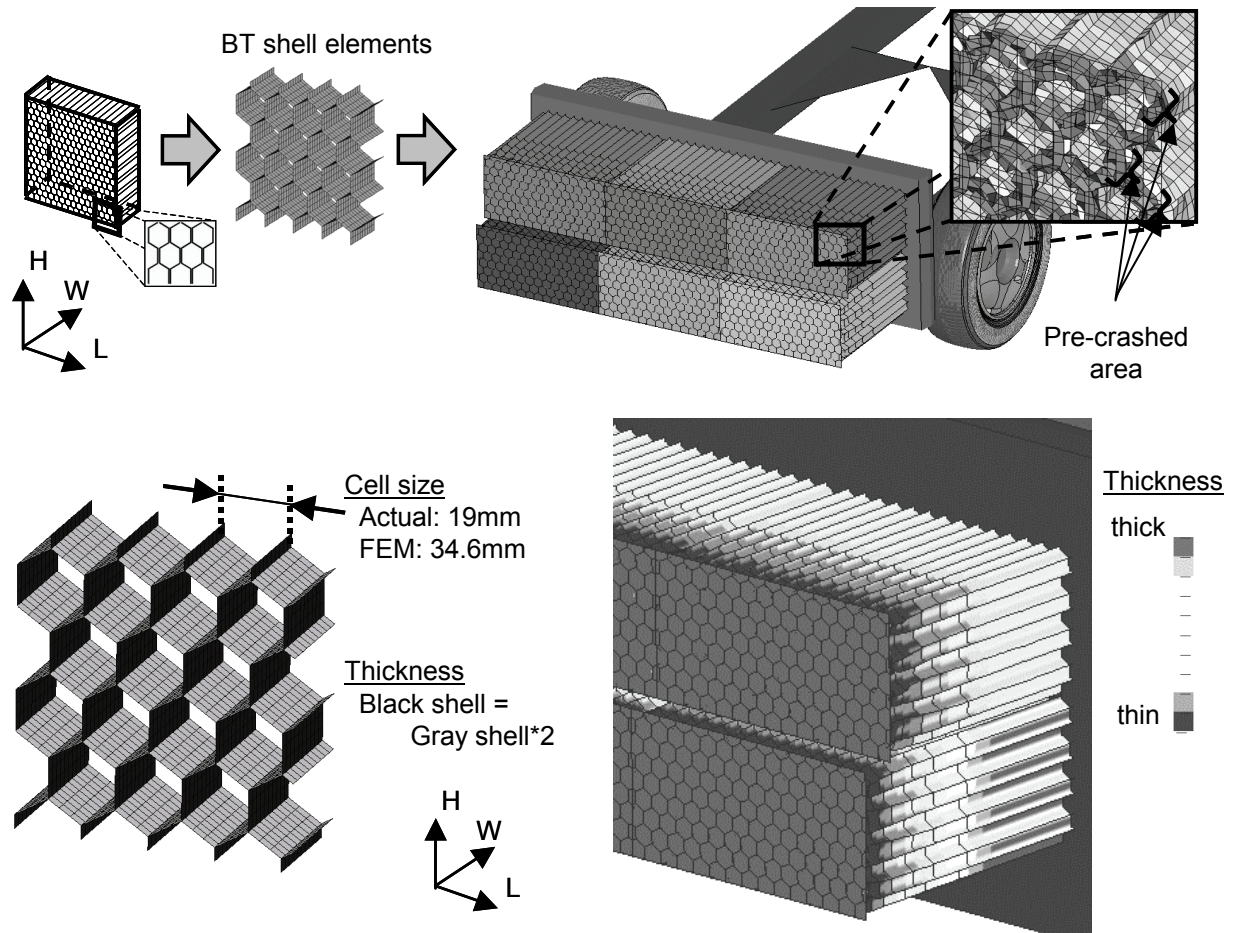


Fig.8 Aluminum honeycomb model using shell elements for ECE R95 MDB model

4 Verification of shell MDB model in barrier impact analyses

4.1 Comparison of test results and FEM analysis for MDB-barrier impacts

To verify the accuracy of the newly created shell element MDB model, FEM analyses were performed on the flat barrier impact and the offset pole impact. Fig.9 (a) shows the relationship between the stroke and the barrier force in the flat barrier impact analysis, and Fig.9 (b) shows them in the offset pole impact analysis.

In the flat barrier impact analysis, the honeycomb compressive strength of the shell element MDB model generally matched the test result, in the same way as the solid element MDB model.

In the offset pole impact analysis, the relationship between the stroke and the barrier force of the shell element MDB model is more precise to the test result than the solid element MDB model and the difference of the stroke with the test result decreased from 32 mm to 3 mm.

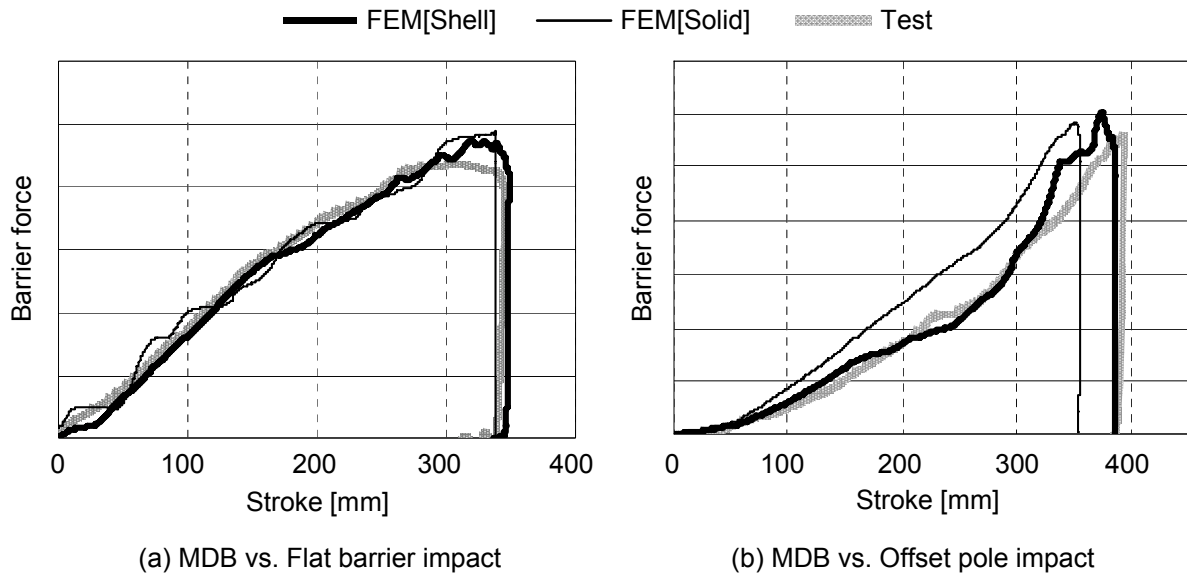


Fig.9 Relationship between the stroke and the barrier force

4.2 Cause of the improved barrier force prediction accuracy in the offset pole impact analysis

This section examines the cause of the improved barrier force prediction accuracy in the offset pole impact analysis with the shell element MDB model. Fig.10 shows the deformed shape of the aluminum honeycomb near the pole, and Fig.11 shows the ratio of the hourglass energy (HE) to the total energy (TE) in the region B.

Compared to the solid element MDB model, the hourglass energy of the shell element MDB model decreased and its ratio to the total energy decreased from 60% to under 10%. Therefore, it is concluded that the honeycomb deformation mode along the pole surface was replicated in shell element MDB model, because non-physical deformation resistance by hourglass control was decreased.

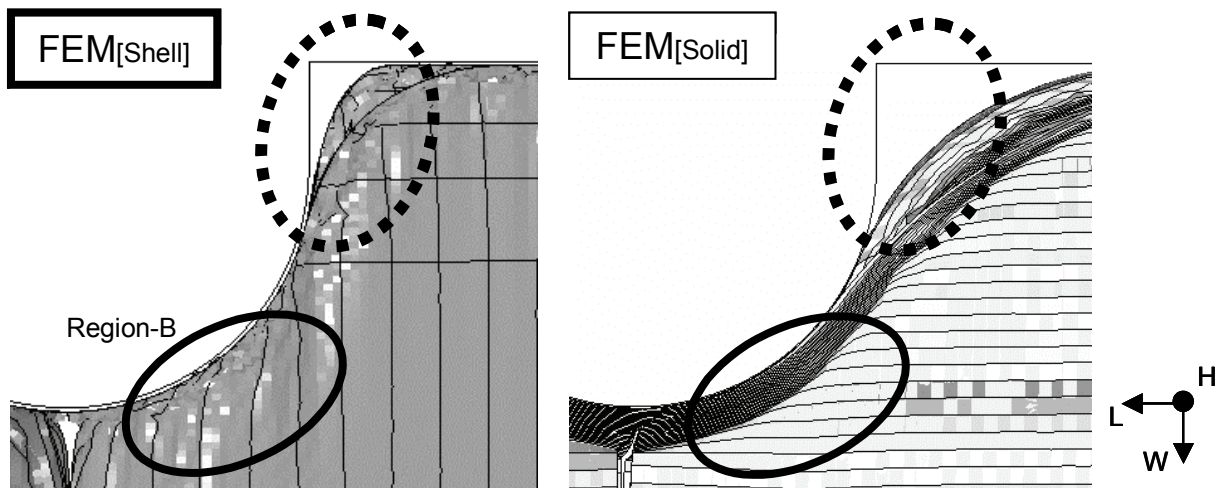


Fig.10 Deformed shape of the aluminum honeycomb near the pole

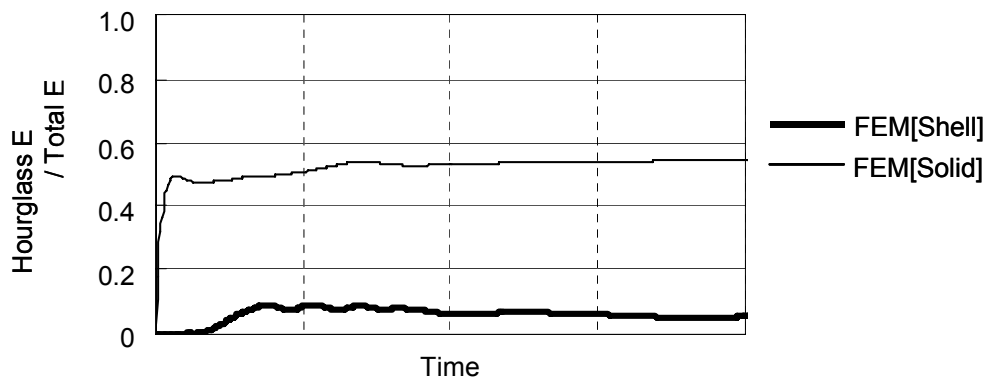


Fig.11 Ratio of the hourglass energy to the total energy in the region B

5 Verification of shell MDB model in full vehicle side impact analysis

5.1 Overview of full vehicle side impact analysis model

Fig.12 shows the ECE R95 side impact analysis model. The vehicle model used in this analysis consisted of 800,000 elements and an ES-2 dummy model was placed on the front seat. Table. 1 shows the hardware that was used and its CPU cost. Simulations were performed on the MPP version, LS-DYNA V970 Revision 5434 using Fujitsu Prime Power (16 CPU). The CPU cost increase was about 20% by using the shell element MDB model, compared to the solid element MDB model.

Table.1 Hardware and CPU cost

	Shell-MDB	Solid-MDB
Hardware	Fujitsu PRIME POWER 16CPU ※MPP LS-DYNA V970rev5434	
CPU cost	1.2	1.0

Shell-MDB model
770,000 elements

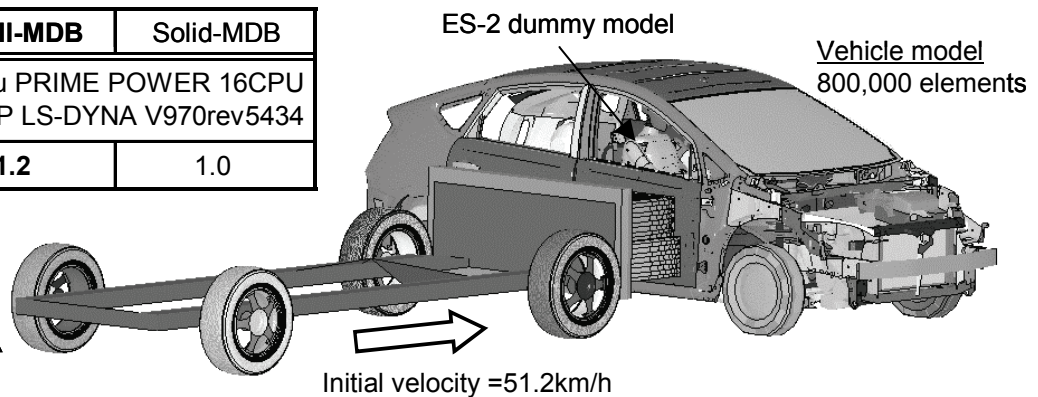
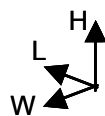


Fig.12 ECE R95 side impact analysis model

5.2 Deformed shapes of the MDB honeycomb and vehicle

Fig.13 shows the deformed shape of the MDB honeycomb, Fig.14 shows the deformed shape of the vehicle and Fig.15 shows the deformed shape of the center pillar. The depression at the lower part of the MDB honeycomb made by the impact of the door beam was accurately replicated in the FEM analysis of the shell element MDB model. The deformed shape of the vehicle in the FEM analysis of shell element MDB model was also more precise to that of the solid element MDB model, and the difference of the front door deformation from the test result decreased from 38 mm to 8 mm. Furthermore, the curved deformation of the center pillar was also closely replicated in the shell element MDB model.

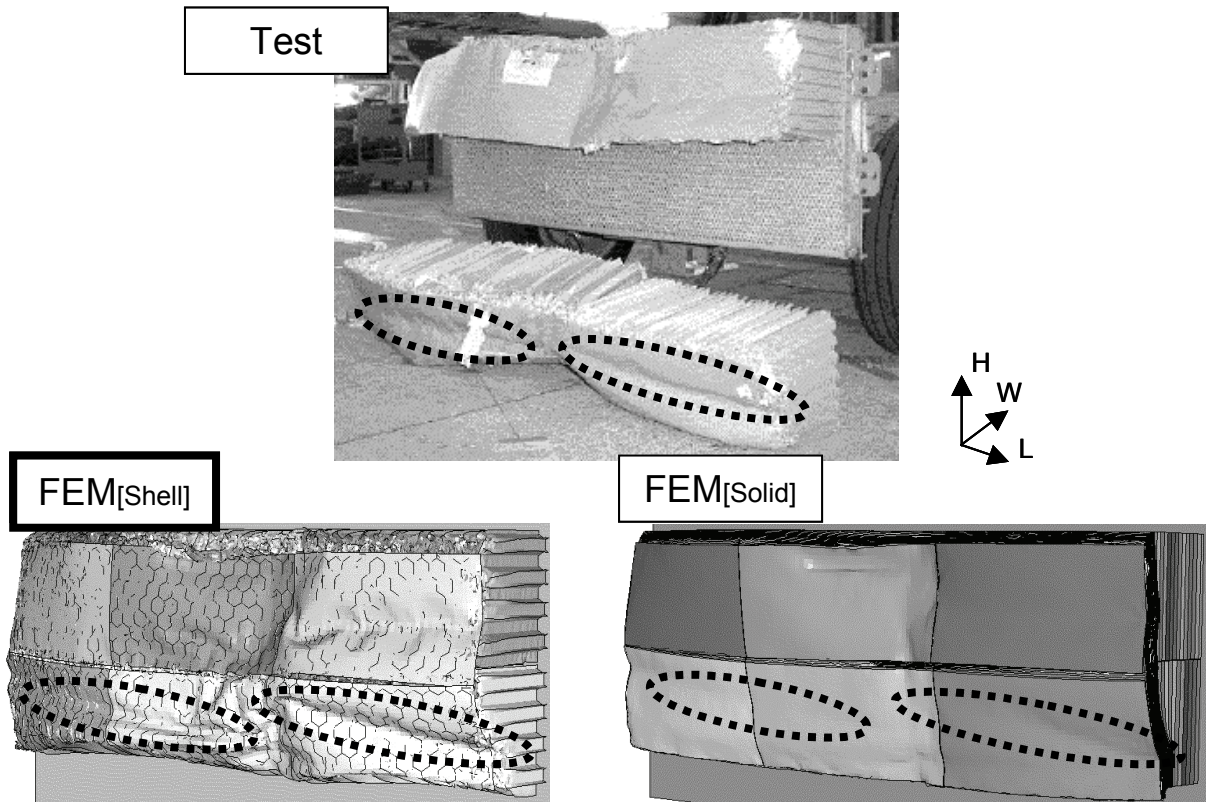


Fig.13 Deformed shape of the MDB honeycomb

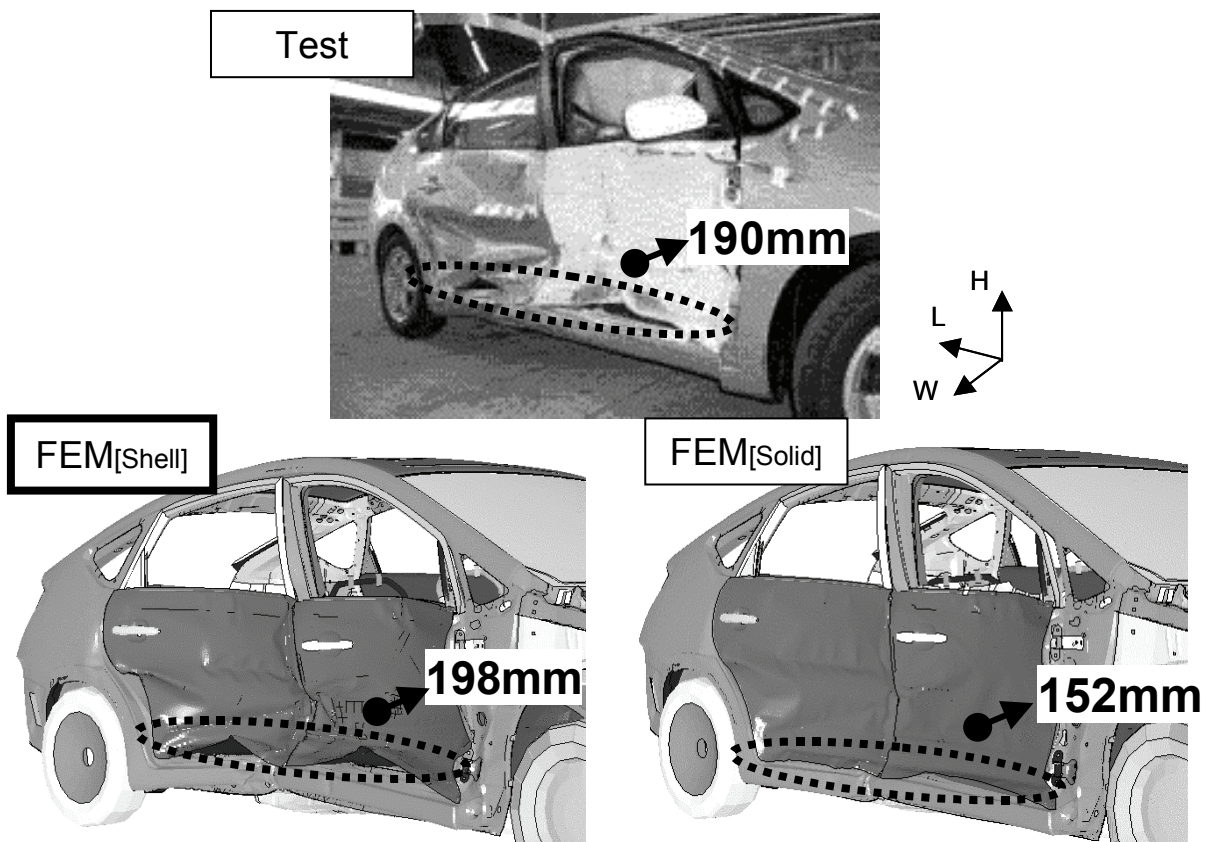


Fig.14 Deformed shape of the vehicle

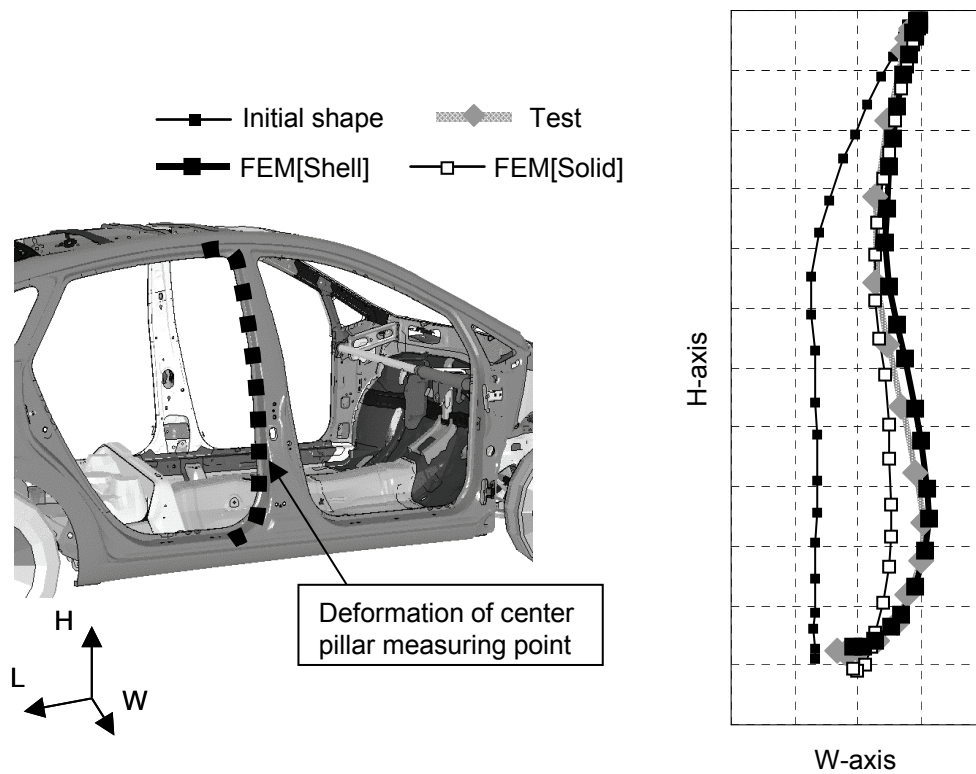


Fig.15. Deformed shape of the center pillar

5.3 Door intruding velocity and dummy injury value

The deformed shapes of the MDB honeycomb and the vehicle have been successfully replicated by the use of the shell element MDB model. Therefore, this section examines in detail the prediction accuracy of the vehicle deformation history and the input force history to the dummy model.

Fig.16 shows the deformed shape of the cross section at the front door intruding velocity measuring point at $t=20$ ms, Fig.17 shows the time history of the front door inner panel velocity and Fig.18 shows the time history of the dummy pelvis force on the front seat.

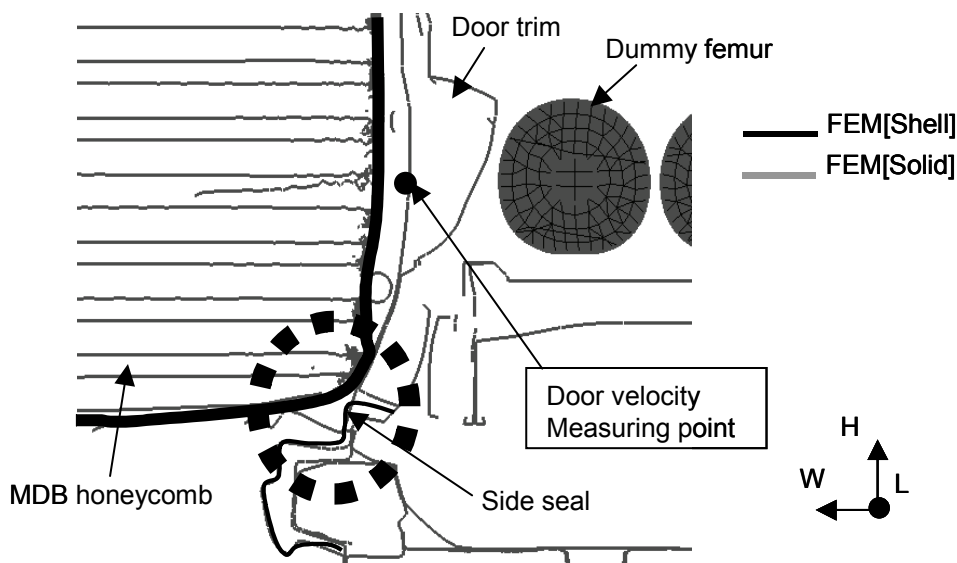


Fig.16 Deformed shape of the cross section at the Fr door intruding velocity measuring point ($t=20$ ms)

In contrast to the side seal of the vehicle preventing the intrusion of the honeycomb of the solid element MDB model, the honeycomb of the shell element MDB model went over the side seal and intruded inside the vehicle. This appears to be due to the decreasing of the deformation resistance by hourglass control of the honeycomb in the collision with the side seal. Thus, the front door intruding velocity peak at $t=20$ ms, where the door trim has impacted the dummy, was replicated and the rise timing of the dummy pelvis force became closer to the test result.

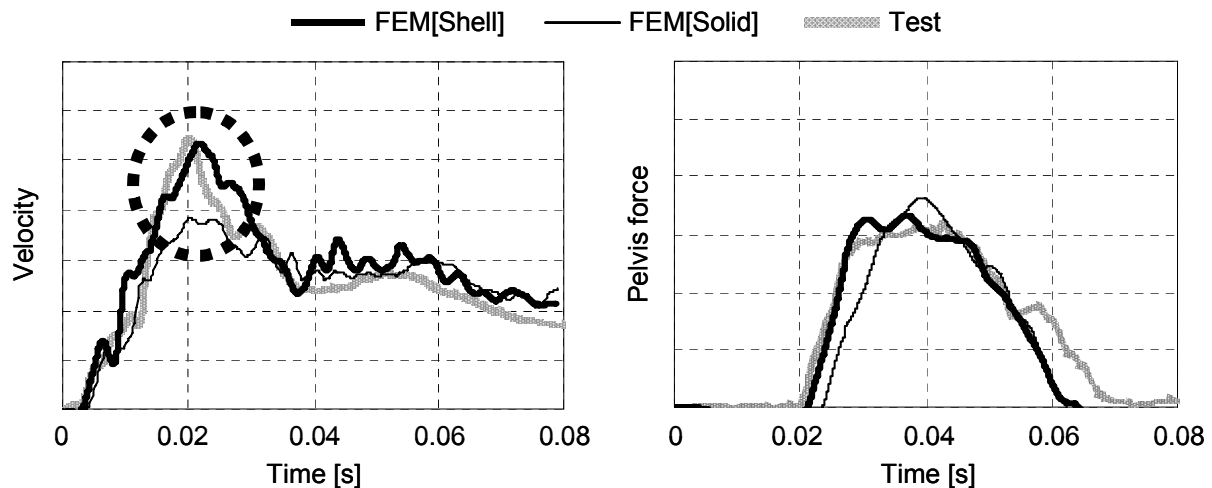


Fig.17 Time history of Fr door intruding velocity

Fig.18 Time history of Fr dummy pelvis force

6 Conclusion

A side impact MDB model using shell elements has been successfully developed. A barrier impact analysis and a full vehicle side impact analysis have been performed using this MDB model. As a result, it was verified that this MDB model is capable of simulating test results for vehicle and MDB deformed shape, and for time histories of barrier force, door velocity and occupant injury value.

Reference

- [1] Dr. Tore Tryland, "Alternative Model of the Offset and Side Impact Deformable Barriers", 9th International LS-DYNA Users Conference, Page. 1-9_1-16
- [2] Shigeki Kojima, "Development of Aluminum Honeycomb Model using Shell Elements", 9th International LS-DYNA Users Conference, Page. 18-1_18-10
- [3] Shigeki Kojima, "A Study on Yielding Function of Aluminum Honeycomb", 5th European LS-DYNA Users Conference, Page. 5b-18
- [4] Moisey B Shkolnikov, "Honeycomb Modeling for Side Impact Moving Deformable Barrier (MDB)", 7th International LS-DYNA Users Conference, Page. 7-1_7-14
- [5] EECV Working Group 13, "Recommendations for a Revised Specification for the EECV Mobile Deformable Barrier Face", Nov.2001, Page. 2_8
- [6] Paul Du Bois, "Crashworthiness Engineering Course Notes"
- [7] J. Hallquist, "LS-DYNA Keyword Users Manual (Update), Version970/Rev5434"